U–Pb zircon geochronology and tectonostratigraphy of southern Liverpool Land, East Greenland: Implications for deformation in the overriding plates of continental collisions

Scott M. Johnston [a,*], Ebbe H. Hartz [b,c], Hannes K. Brueckner [d,e], George E. Gehrels [f]

[a] Physics Department, California Polytechnic State University, San Luis Obispo, CA 93407, USA
[b] Physics of Geological Processes, University of Oslo, P.O. Box 1048 Blindern, NO-0316 Oslo, Norway
[c] Det Norske Oljeselskap, P.O. Box 2070 Vika, NO-0125 Oslo, Norway
[d] Lamont-Doherty Earth Observatory of Columbia University, Palisades, NY 10964, USA
[e] Queens College and the Graduate Center of the City University of New York, Flushing, NY 11367, USA
[f] Department of Geosciences, University of Arizona, Gould-Simpson Building #77 1040 E 4th St., Tucson, AZ 85721, USA

A B S T R A C T

The East Greenland Caledonides formed in the overriding plate as Baltica was subducted westward beneath Laurentia from 460 to 360 Ma, and offer a unique opportunity to investigate lower crustal deformation in the overriding plates of continental collisions. Field work and new zircon geochronology from gneisses in southern Liverpool Land, exposed in the hinterland ~100 km east of the nearest Caledonian gneisses, define three tectonostratigraphic units that are, from the bottom up, the eclogite + peridotite-bearing Tværdal complex and the granulite-facies Jættedal complex in the footwall of the top-N Gubbedalen shear zone, and the Hurry Inlet granite and associated paragneiss screens in its immediate hangingwall. Zircons from Tværdal complex gneisses yield metamorphic rims that cluster in age from 409 to 401 Ma and overgrow magmatic cores of 1674 and 1665 Ma in two samples, and range from ~1800–1000 Ma in a third sample. In contrast, zircons from three samples in the Jættedal complex and two samples in the paragneiss screens of the Hurry Inlet granite yield metamorphic rims that cluster in age from 438 to 417 Ma with Archean–Early Neoproterozoic detrital cores. A cross-cutting granitic dike in the Jættedal complex yields an age of 394 Ma. Archean–Early Neoproterozoic detrital zircons associated with ~440–420 Ma metamorphism in the Liverpool Land paragneisses suggests correlation with the Krummedal sequence and the Hagar Bjerg thrust sheet of Laurentian affinity. 1670 Ma cores in the Tværdal complex, and ~400 Ma eclogite-facies metamorphism, allow correlation of the Tværdal complex with the Western Gneiss Region in Norway, and it may therefore be of Baltican affinity. Furthermore, the contact between the older Jættedal complex with the younger Tværdal complex requires the existence of a structure, named the Ittoqqortoormiit shear zone herein, which juxtaposed these rocks prior to the initiation of normal-sense slip along the Gubbedalen shear zone. This work provides geochronologic evidence for continental underplating of the overriding plate by the subducting plate during orogenesis, and supports models for high-pressure exhumation in continental collisional settings that identify separate structures associated with initial emplacement in the lower–middle crust and subsequent upper-crustal exhumation.

1. Introduction

Deformation in the overriding plates of continental collisions is characterized by complex feedback mechanisms between contraction and extension that have regional implications for collisional dynamics and long-term lithospheric structure and composition (e.g., Molnar and Tapponnier, 1975). To a large degree, the balance between contraction and extension is controlled by processes affecting the strength and style of deformation in the mid–lower crust including foundering of lithospheric roots, lower crustal flow, and continental underthrusting by the lower plate (e.g., Barazangi and Ni, 1982; England and Houseman, 1989; Bird, 1991). In addition to the specific predictions that each of these processes makes for the thermomechanical evolution of orogenic belts, the discovery of continental crust >90 km thick beneath Tibet (Wittlinger et al., 2004) and ultrahigh-pressure rocks exhumed in the overriding plate of the Caledonian orogen (Gilotti and Krogh Ravna, 2002; Gilotti and McClelland, 2007) highlight the relevance of deformation in the overriding plate with respect to the formation and exhumation of ultrahigh- and high-pressure terranes. The presence of high-pressure rocks in

the overriding plates of continental collisions challenges accepted models for their formation and exhumation along subduction interfaces (e.g.,Ernst et al., 2007), while thermomechanical (Gerya et al., 2008; Warren et al., 2008) and petrological (Hacker et al., 2005) models that suggest continental underplating and exhumation in the overriding plate have significant implications for the nature of crust–mantle interactions and the composition of continental crust. Despite this growing body of literature, crucial petrologic and structural relationships from the lower crust remain buried in recent and active orogens, and models for the deep burial and subsequent exhumation of continental crust in the overriding plate need to be supplemented by observations from ancient analogues that expose deeper crustal sections of orogens.

In this paper, we investigate mid–lower crustal tectonostratigraphic relationships from East Greenland that formed in the overriding plate of the Caledonian orogen. The Caledonides formed as Baltica and Laurentia collided with each other during closure of the Iapetus Ocean, and culminated with the subduction of Baltica beneath the Laurentian margin (Gee, 1975; Roberts, 2003). The Scandinavian Caledonides are marked by eastward thrusting and sequential stacking of allochthonous and para-autochthonous nappes onto the Baltican margin during the Silurian (Brueckner and van Roermund, 2004), and terminated with the subduction of Baltican crust and its assembled outboard nappes to mantle depths by 415–400 Ma (Carswell et al., 2003; Root et al., 2004) and subsequent rapid exhumation through muscovite closure by 400–380 Ma (Walsh et al., 2007). Across the Atlantic, the Greenland Caledonides consist of rocks of Laurentian affinity that were situated in the overriding plate of the Caledonian orogen (Haller, 1971; Henriksen, 1985). Mid–lower crustal rocks currently exposed within the Greenland Caledonides indicate early crustal thickening, widespread anatexis and at least two pulses of late- to postorogenic extension (Jones and Strachan, 2000; Hartz et al., 2001; White and Hodges, 2002; McClelland and Gilotti, 2003; Gilotti and McClelland, 2008), and represent an ancient analogue to the overriding plate of the active Himalaya–Tibet orogen. Using U–Pb zircon geochronology on gneisses from southern Liverpool Land, East Greenland, we explore first order questions including the continental affinity, provenance and timing of metamorphism in the hinterland of the southern Greenland Caledonides. Our results define the tectonostratigraphy of southern Liverpool Land, and suggest 1) at least partial underplating of the Laurentian overriding plate by subducted continental crust of Baltican affinity during Caledonian orogenesis, (Augland, 2007), and 2) subsequent, multi-stage exhumation of deeply-buried rocks via two distinct structures related to tectonic underplating and crustal exhumation, respectively.

2. Regional geology: the Greenland Caledonides

The Greenland Caledonides can be split into northern and southern sections based on structural and metamorphic patterns (Gilotti et al., 2008). North of 76°N, the orogen consists of several westward-propagating thrust sheets that grade from unmetamorphosed sedimentary rocks and greenschist-facies rocks in the structurally lowest thrust sheets in the west, through amphibolite, and ultimately eclogite-facies rocks preserved in the structurally highest thrust sheets in the east (Higgins et al., 2004; Gilotti et al., 2008). Structurally highest, the North-East Greenland eclogite province is characterized by eclogite-facies metamorphism at ~400 Ma (Gilotti et al., 2004), and in its easternmost exposures, UHP metamorphism at ~360 Ma (McClelland et al., 2006), and was at least partially exhumed through dextral transpression and amphibolite-facies strike–slip shear zones active throughout the Devonian and Early Carboniferous (Sartini-Rideout et al., 2006). South of 76°N, the thrust architecture of the northern Greenland Caledonides is complicated by a variety of syn-postorogenic normal faults (Fig. 1). Despite this extensional dissection, four tectonostratigraphic units can be identified in the southern Greenland Caledonides. From the bottom up, these include the Foreland, the Niggli Spids Thrust Sheet (NSTS), the Hagar Bjerg Thrust Sheet (HBTS), and the Franz Joseph Allochthon (Hartz et al., 2001; Henriksen, 2003; Higgins et al., 2004). The structurally lowest Foreland is exposed in the far western regions of the orogen and in windows through structurally-higher thrust sheets in the cores of several anticlinal structures. The Foreland consists of Archean–Paleoproterozoic gneisses depositionally overlain by Paleoproterozoic–Ordovician sedimentary rocks (Higgins et al., 2001) that display low-greenschist-facies Caledonian metamorphic textures (Leslie and Higgins, 1999).

The Foreland is overthrust by the NSTS and the structurally-higher HBTS, both of which are composed of Archean–Paleoproterozoic crystalline basement orthogneiss complexes overlain by the Meso-Neoproterozoic Krummedal sequence paragneisses (Higgins et al., 2004). As an alternative to thrust sheet imbrication, it has also been proposed that these two units may represent duplication of the same basement–cover pair in a recumbent fold within a single thrust sheet (Haller, 1971; Andresen et al., 2007). Regardless of the nature of the NSTS–HBTS contact, significant differences in metamorphic and exhumation histories make their distinction useful for determining structural position within the regional tectonostratigraphy. First, based on the correlation of Payer Land basement with the NSTS (Higgins et al., 2004; Gilotti et al., 2008), peak metamorphic conditions recorded in mafic pods and anatectic paragneisses within the NSTS reached high-pressure granulite-facies metamorphic conditions (1.4–1.7 GPa at 800–850 °C, Elvevold et al., 2003; Gilotti and Elvevold, 2002), which contrast with generally lower-pressure granulite-facies metamorphic conditions in the HBTS (~1.0 GPa at 785–915 °C, Jones and Escher, 2002; Jones and Strachan, 2000; Kalsbeek et al., 2001; White and Hodges, 2003). Second, the NSTS underwent peak metamorphism at ~405 Ma (McClelland and Gilotti, 2003), whereas ages for peak metamorphism, migmatization, and granite emplacement in the HBTS range from 445 to 420 Ma (Strachan et al., 1995; Watt et al., 2000; Hartz et al., 2001; Kalsbeek et al., 2001).

The overlying Franz Joseph Allochthon consists of a thick succession of Neoproterozoic–Ordovician sedimentary rocks that increase in metamorphic grade from unmetamorphosed sedimentary rocks in the uppermost levels through regionally developed garnet–sillimanite-bearing pelites (Smith and Robertson, 1999) that are locally intruded by ~430 Ma granites above the contact with the HBTS (Kalsbeek et al., 2001; Andresen et al., 2007). The top of the East Greenland tectonostratigraphic section consists of Middle Devonian–Carboniferous fault-bounded sedimentary basins that locally rest unconformably on the Franz Joseph Allochthon and the underlying thrust sheets.

Emplacement of the southern East Greenland thrust sheets was accompanied by several generations of repeatedly reactivated syn-late-orogenic extensional detachments (Hartz et al., 2000; Gilotti and McClelland, 2008). Early extension-related exhumation associated with normal-sense displacement between the HBTS and the Franz Joseph Allochthon is documented by a metamorphic discontinuity between the two units and by ~425 Ma U–Pb monazite ages from syn-kinematic leucosomes in the HBTS (White et al., 2002). These two units were subsequently juxtaposed while in the middle crust and exhumed together through muscovite closure to Ar by 423–414 Ma (White and Hodges, 2002). In contrast, high-P granulite-facies metamorphism at ~405 Ma (McClelland and Gilotti, 2003) in the NSTS, a muscovite cooling age of ~380 Ma (Hartz et al., 2000), and 69 K–Ar biotite ages of <405 Ma from Suess Land (Rex and Higgins, 1985) indicate a second stage of extensional deformation associated with low-angle normal-sense detachments that exhumed the youngest and deepest sections of the orogen (White and Hodges, 2002). These detachment structures consistently display normal-sense displacement, although kinematic indicators variably exhibit both top-E, orogen-normal (Hartz and Andresen, 1995), and top-SW,

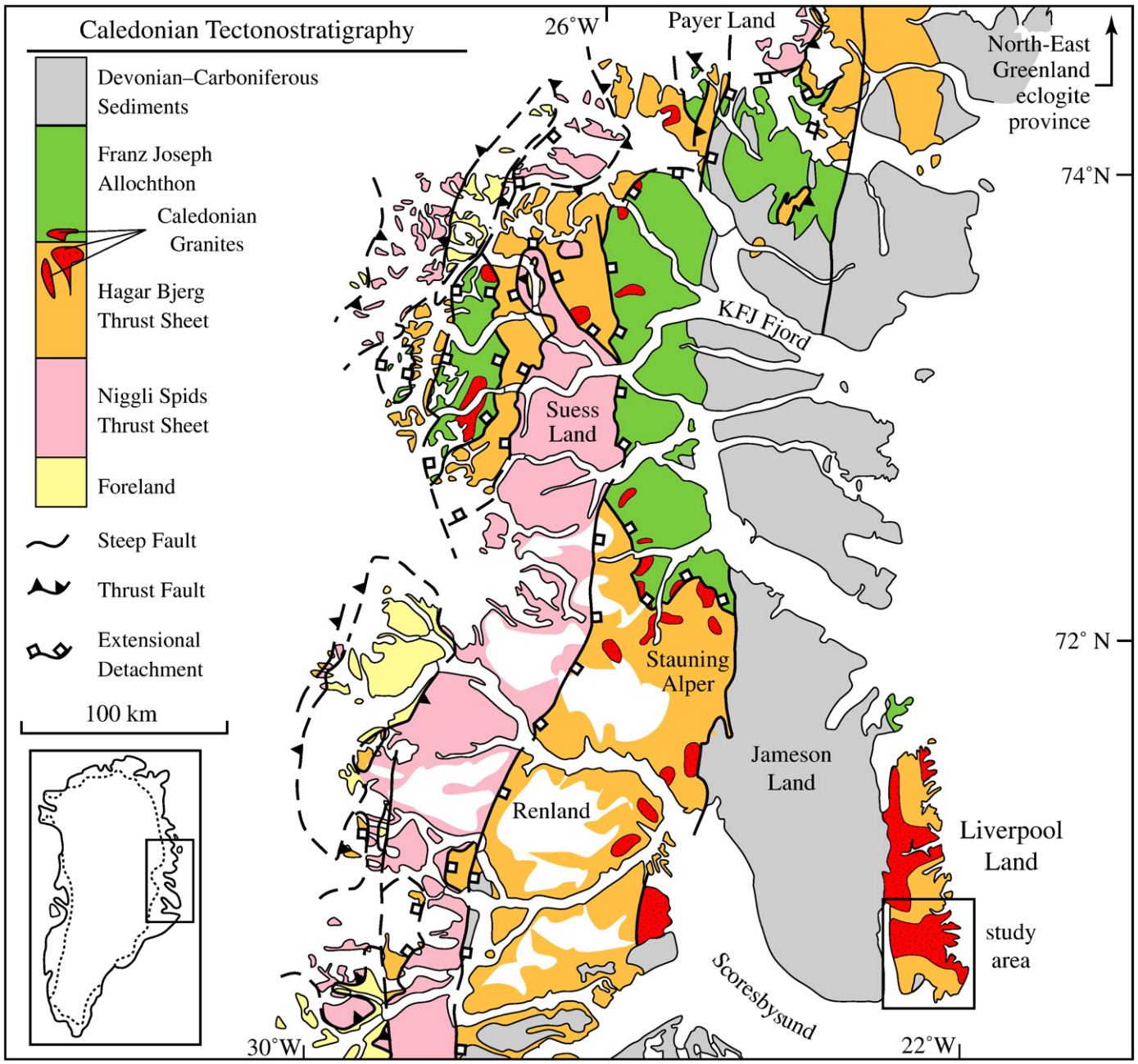

Fig. 1. Regional geologic map of the southern Greenland Caledonides showing the location of the Liverpool Land study area with respect to the tectonostratigraphy of the inland fjords. Tectonostratigraphy after Higgins, et al. (2004), fault relationships after Gilotti and McClelland (2008). KFJ Fjord–Kejser Franz Joseph Fjord.

orogen-parallel displacement (Jones and Strachan, 2000; Gilotti and Elvevold, 2002). Farther east, the distinction in exhumation age between the HBTS and the NSTS may break down as several studies reveal migmatite-bearing units correlated with the HBTS that yield ages for muscovite closure through Ar<400 Ma (Dallmeyer et al., 1994; Bowman, 2008).

Liverpool Land, separated from the nearest high-grade Caledonian thrust sheets 100 km to the west by unmetamorphosed Devonian–Carboniferous sedimentary rocks (Fig. 1), consists of high-grade gneiss complexes and Caledonian calc-alkaline granites that are most completely exposed near the southern tip of the peninsula (Coe, 1975; Friderichsen and Surlyk, 1981; Cheeney, 1985; Bengaard and Watt, 1986). The Liverpool Land gneisses are tentatively correlated with the HBTS based on their association with Caledonian granites (Higgins et al., 2004). However, the identification of eclogites and garnet peridotites boudins within orthogneisses in southwest Liverpool Land (Krank, 1935; Smith and Cheeney, 1981; Hartz et al., 2005) suggests that at least some

Fig. 2. A) Geologic map of Liverpool Land illustrating the regional geology and relative location of the Kalkdal paragneiss samples with respect to the gneiss complexes of southern Liverpool Land. B) Detailed geologic map of southern Liverpool Land illustrating petrologic and structural relationships, and sample locations from the Tværdal and Jættedal complexes. C) Cross section illustrating structural relationships in southern Liverpool Land. Maps modified from Friderichsen and Surlyk (1981) based on new mapping and geochronology from this study. JG–Jættedal Glacier; TG–Trefoden Glacier, N–Nissedal, * in the cross section indicates weakly developed top-S to top-SW shear fabrics below the Gubbedalen shear zone (this study, Augland, 2007).

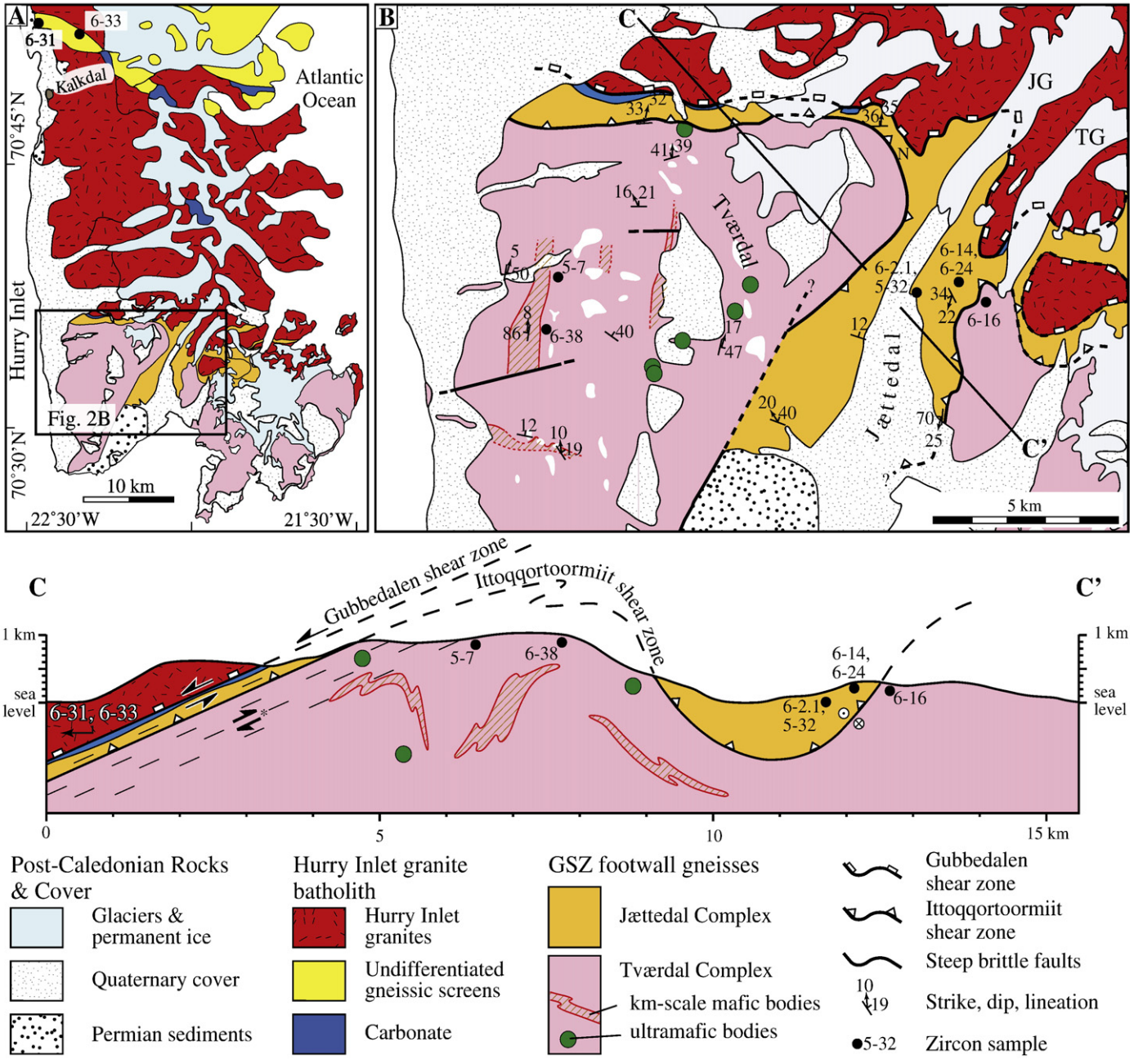
A
6-31
6-33
Kalkdal
Atlantic Ocean
70°45'N
70°30'N
Hurry Inlet
Fig. 2B
10 km
22°30'W
21°30'W
B
C
C'
JG
TG
Tværdal
Jættedal
6-14, 6-24
6-2.1, 5-32
6-16
6-38
5-7
5 km
C
C'
Gubbedalen shear zone
Ittoqqortoormiit shear zone
1 km
sea level
6-31, 6-33
0
5
10
15 km
Post-Caledonian Rocks & Cover
Glaciers & permanent ice
Quaternary cover
Permian sediments
Hurry Inlet granite batholith
Hurry Inlet granites
Undifferentiated gneissic screens
Carbonate
GSZ footwall gneisses
Jættedal Complex
Tværdal Complex
km-scale mafic bodies
ultramafic bodies
Gubbedalen shear zone
Ittoqqortoormiit shear zone
Steep brittle faults
Strike, dip, lineation
Zircon sample

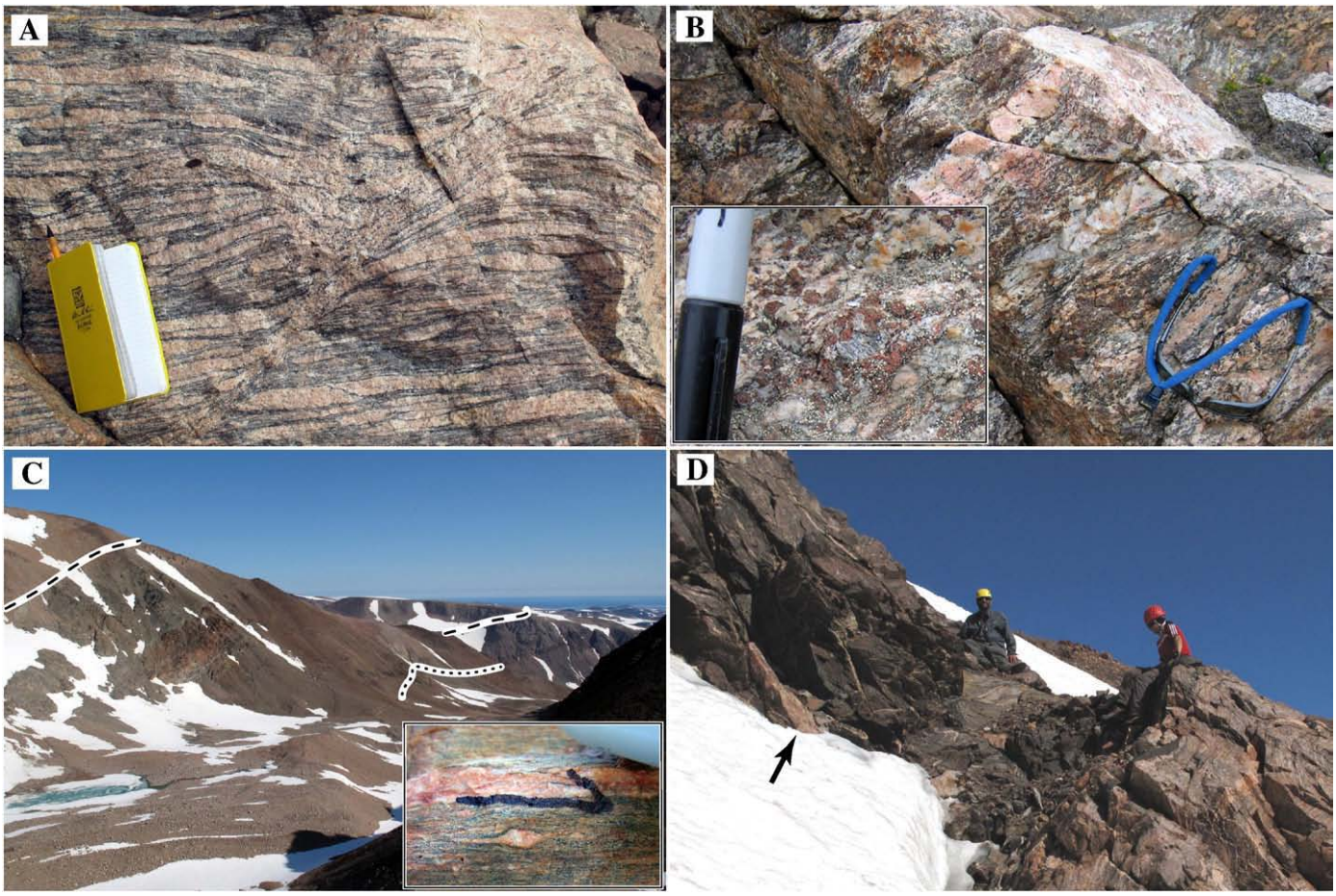

Fig. 3. Field photos from southern Liverpool Land. A) A migmatitic orthogneiss common throughout the Tværdal complex suggesting syn-deformational melting. B) A typical paragneiss outcrop within the Jættedal complex illustrating garnet + kyanite + biotite + plagioclase gneiss (representative of sample 6-2.1) interlayered with concordant leucocratic melts (representative of sample 5-32); inset displays a close-up view of the paragneiss. C) Looking along strike of the Gubbedalen shear zone eastward down the axis of Nissedal and across Jættedal where the shear zone can be seen high on the valley walls above the Jættedal Glacier. The approximate location of the uppermost detachment surface is marked with a dashed line, and the location of the Tværdal–Jættedal contact imaged in Fig. 3D is indicated with the dotted line. The inset image displays a ductilely deformed feldspar porphyroclast from the Tværdal complex within the shear zone demonstrating amphibolite-facies, top-N (030) slip; the arrow is ~2 cm in length. D) The contact between the Tværdal complex orthogneisses (structurally low, lighter rocks) and Jættedal complex biotite + garnet + kyanite gneisses (structurally high, darker rocks) on the northern wall of Nissedal and ~200 m below the Gubbedalen shear zone detachment surface. The nearly vertical granitic dikes that cut foliation in the Jættedal rocks (indicated with arrow) are similar to sample 6-24.

of the rocks within the Liverpool Land area may be representative of either the NSTS (Gilotti et al., 2008) or a fragment of subducted continental crust with Baltican affinity (Augland, 2007). Importantly, the relative eastward location of the Liverpool Land gneisses provides a glimpse of the deepest levels of the hinterland of the Greenland Caledonides, and offers a new perspective on the evolution of the overriding plate of the Caledonian orogen.

3. Liverpool Land geology

The Liverpool Land tectonostratigraphy is divided into three distinct units based on field mapping of petrologic and structural observations, and on zircon geochronology (see below). From the bottom up, they are the Tværdal and Jættedal complexes in the footwall of the Gubbedalen shear zone (GSZ), and the Hurry Inlet granite in the hanging wall of the GSZ (Fig. 2).

3.1. Tectonostratigraphic unit descriptions

Structurally lowest, the Tværdal complex consists of orthogneisses along the southern coast of Liverpool Land that include abundant mafic, and rare ultramafic bodies to the west of Jættedal (Fig. 2). Host orthogneisses are characterized by a variety of granitic–granodioritic compositions with amphibolite-facies mineral assemblages, although pervasively developed migmatitic textures (Fig. 3A) and widespread relict clinopyroxene attest to earlier equilibration at high-T conditions. Kilometer- to m-scale mafic bodies west of Jættedal commonly display cm-scale monomineralic layering and compositional banding. Eclogite-facies metamorphism has been dated to 393–399 Ma (Hartz et al., 2005; Augland, 2007), while peak mineral assemblages in eclogite yield *P–T* estimates of >18.2 kbar at T>800 °C (Hartz et al., 2005; Buchanan, 2008). Furthermore, variably-serpentinized, Cr-rich garnet peridotite lenses suggest tectonic emplacement and burial of the Tværdal complex to mantle depths (Smith and Cheeney, 1981). Two generations of post-peak melts within the Tværdal complex yield U–Pb zircon TIMS ages of 388–385 Ma (Hartz et al., 2005; Augland, 2007), and include hornblende pegmatites that are abundant within mafic boudin necks and melt pods concordant to regional foliation, and steeply-dipping granitic dikes that cut sharply across all other compositions and foliations. Continuous mapping of the Tværdal complex to the east of Jættedal is obscured by brittle faulting and alluvial cover, although unique zircon age characteristics (see zircon geochronology below) allows correlation of relatively monotonous hornblende-bearing granodioritic gneisses east of Jættedal with the Tværdal complex. In contrast to outcrops farther west, rare mafic

boudins in the Tværdal complex east of Jættedal contain only amphibolite-facies mineral assemblages.

The Jættedal complex structurally overlies the Tværdal complex, and consists of pelitic schists, gneisses and calc-silicates interlayered with granodioritic–dioritic orthogneisses. Pelitic assemblages within the Jættedal complex include garnet + kyanite + biotite + plagioclase + rutile + quartz ± K-feldspar (no muscovite) that suggest granulite-facies metamorphic conditions. Both paragneiss and orthogneiss compositional layers are characterized by migmatitic textures that range from nebulitic migmatites that feed concordant granitic dikes in pelitic rocks (Fig. 3B) to stromatic migmatites. The Jættedal complex is also cut by discordant syn-post kinematic granitic dikes and veins similar to the late-stage granitic dikes within the Tværdal complex (Fig. 3D).

Structurally above the Tværdal and Jættedal complexes, the hangingwall of the GSZ is composed of the Hurry Inlet granite and associated supracrustal screens (Coe, 1975). The Hurry Inlet granite consists of a collection of high-K granites and granodiorites that plot along a calc-alkaline trend (Coe, 1975) and were intruded in several pulses from 445 to 423 Ma (Hartz et al., 2005; Augland, 2007). In contrast to exposures in the Tværdal and Jættedal complexes, the Hurry Inlet granites are generally undeformed and lack well-developed foliations other than local magmatic structures. This intrusive complex is also characterized by rare screens and enclaves that have been incorporated into the batholith from the country rock (Coe, 1975). The largest of these screens strikes E–W across Liverpool Land and is composed of foliated carbonates, pelitic schists and garnet + K-feldspar + plagioclase + quartz ± kyanite/sillimanite ± muscovite gneiss.

3.2. Tectonostratigraphic contact relationships

Generally N–S-striking foliations and weakly developed N–S trending lineations observed in both the Tværdal and Jættedal complexes are progressively transposed into the shallowly N-dipping GSZ (Cheeney, 1985, Figs. 2, 3C). North of Tværdal and in Nissedal, fabrics associated with the GSZ increase from discontinuous outcrop-scale shear zones at lower structural levels to complete transposition of earlier foliation and layering in the several hundred meters below the detachment surface. Within the uppermost 100–200 m of the GSZ, N-trending stretching lineations and asymmetric shear-sense indicators including sigma clasts, S–C fabrics, asymmetric boudinage, and C′ shear bands indicating top-N displacement are pervasively developed. Ductile displacement along the GSZ was initiated at amphibolite-facies temperatures, as indicated by ductile deformation in feldspar (Fig. 3C), whereas widespread growth of chlorite and late brittle fracture in feldspar indicate continued top-N displacement through greenschist-facies temperatures. The detachment surface itself is delineated by greenschist-facies ultramylonites and breccias associated with discontinuous carbonate lenses and stringers up to 20 m thick. In the vicinity of Tværdal, the top-N fabrics of the GSZ overprint a variety of older fabrics in the Tværdal complex including top-S (Augland, 2007), top-SW and symmetric shear fabrics. Along strike to the east, the detachment surface and top-N shear fabrics of the GSZ can be mapped visually in high cliffs above the Jættedal Glacier and in outcrop above the Trefoden Glacier (Fig. 2), and top-N shear fabrics are displayed in isolated N-dipping shear zones up to a kilometer below the detachment in granitic dikes that cut foliation in the Jættedal complex.

The structurally lower contact between the Tværdal and Jættedal complexes is marked by a sharp change in rock type from Tværdal complex orthogneisses to Jættedal complex paragneisses, and is concordant to regional foliation (Fig. 3D). North of Tværdal, this contact is strongly overprinted by top-N fabrics of the GSZ. Farther east, the contact emerges into the footwall of the GSZ, wraps around a N-plunging syncline, and is exposed along the eastern wall of Jættedal. Here, amphibolite-facies stretching lineations and top-S/sinistral shear fabrics are weakly developed and there is no evidence for brittle faulting or greenschist-facies deformation along the contact.

4. Liverpool Land zircon geochronology

U–Pb zircon geochronology was performed on eight gneisses and one syn-post kinematic granite using a New Wave Instruments 193 nm ArF excimer laser coupled with a GV Instruments Isoprobe at the Arizona LaserChron Center (University of Arizona, Tucson, AZ) to better define the provenance and metamorphic history of the various Liverpool Land gneisses. Due to the fine size (diameter of 30–150 μm) and intricate chemical zoning observed in CL and in U/Th ratios in many of the analyzed zircons, the small-volume laser ablation multicollector ICP-MS technique of Johnston et al. (2009) was used to delineate core and rim ages for analyzed zircons. With a 10 μm beam set for 32 pulses at 4 Hz yielding a sample pits of ~12 μm in diameter by 3.2 μm deep, between two and 36 analyses on each grain were made using CL images to guide spot placement from rim to core chemical zones, respectively. Rim ages were calculated by pooling analyses with $^{206}Pb/^{238}U$ and $^{207}Pb/^{235}U$ ages < 500 Ma from all analyzed grains within each sample, using the *TuffZirc* algorithm of Ludwig (2003) to trim statistical outliers resulting from either Pb loss or inheritance, and calculate statistically robust $^{206}Pb/^{238}U$ ages. Upper-intercept ages are model 1 solutions to the concordia intercept algorithm of Ludwig (2003) with an anchor at the previously defined rim age, and calculated from analyses with $^{206}Pb/^{238}U$ ages > 500 Ma from individual grains in detrital samples, or from analyses older than 500 Ma from all grains in samples with magmatic protoliths. Analyses that plot off well-defined mixing lines were assumed to be either bad analyses or contaminated with common Pb, and were visually trimmed. To increase counting statistics in detrital samples, after fully mapping cores and rims in 10 grains, additional grains were characterized with single rim and core analysis, and yield poorly constrained upper-intercept ages that are noted separately in detrital age histograms. Upper-intercept and rim age errors are reported at the 95% confidence level (1.96σ) and include analytical errors added in quadrature to systematic errors associated with uncertainty on the U decay constants, the age of the external standard, and the average uncertainty on the analysis session fractionation correction. 96 analyses of secondary standard R33 (419.3 Ma, Black et al., 2004) run throughout the analysis sessions yield a $^{206}Pb/^{238}U$ weighted average age of 418.4 ± 6.6 Ma, and provide a quantitative estimate for the accuracy of the results. Representative CL images and spot analyses are displayed in Fig. 4; CL images and U–Th–Pb data from all grains and analyses are available in the data repository (Tables ES1–10, Figs. ES1–9).

4.1. Tværdal complex

Three gneiss samples from the Tværdal complex were analyzed: samples 5-7 and 6-38 from west of Tværdal and 6-16 from east of Jættedal (Fig. 5). Sample 5-7 is a felsic gneiss adjacent to an eclogite boudin with a foliation defined by K-feldspar + plagioclase + quartz + amphibole and relict garnet and clinopyroxene. Separated zircons are prismatic to rounded, 75–100 μm in diameter, and in CL, they display homogenously dark rims and oscillatory zoning in bright, poorly preserved cores. Rims are characterized by an average U/Th ratio of 33, and 43 of 66 analyses accepted by *TuffZirc* yield a $^{206}Pb/^{238}U$ age of $404.7 + 4.8/-7.0$ Ma. Zircon cores are strongly discordant and analyses from six grains with U/Th ratios < 5 suggest older core populations with upper intercepts that range from ~1800–1000 Ma.

Sample 6-38 is a stromatic migmatite gneiss (Fig. 3A) found throughout the Tværdal complex, and consists of plagioclase + K-feldspar + quartz + biotite ± amphibole ± garnet melanosomes and plagioclase + K-feldspar + quartz leucosomes. Zircons separated

from the bulk rock are prisms up to 200 μm in length that display dark oscillatory zoning in cores, and bright rims typically < 5 μm thick in CL. Despite the fine rim morphology, five rim analyses with an average U/Th ratio of 13.5 from two grains yielded concordant results within 2σ. Although the *TuffZirc* algorithm requires more than 6 ages, a $^{206}Pb/^{238}U$ weighted average age of 403.4 ± 7.3 Ma was calculated from these analyses. 58 analyses from 15 grains with an average U/Th ratio of 5.3 fall on a single mixing line that defines an upper-intercept age of 1674 ± 28 Ma.

Sample 6-16 is an amphibole-bearing granodioritic gneiss that is the dominant rock type within the Tværdal complex east of Jættedal. Separated zircons are prismatic crystals up to 150 μm in length, and in CL, display bright, oscillatory zoning in cores and dark, homogenous rims up to 20 μm thick that are best developed on prism tips. Zircon rims indicate an average U/Th ratio of 316, and 48 of 69 analyses accepted by *TuffZirc* indicate a $^{206}Pb/^{238}U$ age of 408.8 + 5.7/−5.4 Ma. 76 analyses from zircon mantles and cores in 11 grains fall on a single mixing line indicating an upper-intercept age of 1665 ± 22 Ma, and nearly concordant analyses from zircon cores indicate U/Th ratios of 1–2.

4.2. Jættedal complex

Zircons from two paragneisses, one concordant leucocratic melt, and one discordant cross-cutting granitic dike were analyzed from the Jættedal complex (Figs. 6, 8, Table 1). Sample 6-2.1 is a kyanite + garnet + biotite + plagioclase + quartz gneiss with nebulous migmatitic textures (Fig. 3B). Separated zircons are rounded, vitreous beads 30–80 μm in diameter, and CL imaging reveals homogenously bright rims up to 20 μm thick with a variety of bright–dark relict cores displaying oscillatory zoning. Zircon rims yield an average U/Th ratio of 31 and a *TuffZirc* $^{206}Pb/^{238}U$ age of 434.7 + 10.3/−6.2 Ma was calculated from 36 of 57 rim analyses. Detrital cores typically have U/Th ratios < 10; 11 of 15 analyzed grains indicate Archean upper-intercept ages while the remaining 4 grains have Mesoproterozoic upper intercepts that range from 1145 to 1651 Ma.

Sample 5-32 is a foliated leucocratic melt interlayered with sample 6-2.1 that is composed of K-feldspar + plagioclase + quartz and relict garnet that increases in abundance toward the melt layer margins (Fig. 3B). Rounded to prismatic zircons from 30 to 100 μm in length and are characterized by CL images that reveal rare relict cores < 30 μm in diameter overgrown by dark mantles and medium-bright rims exhibiting homogenous to sector chemical zoning. 57 of 78 analyses from dark mantles and brighter rims with U/Th ratios typically < 10 yield a *TuffZirc* $^{206}Pb/^{238}U$ age of 438.0 + 10.5/−9.6 Ma. Due to the relict nature of the cores, only two Archean and two Mesoproterozoic (~1300 and ~1000 Ma) upper-intercept ages, all with U/Th ratios also < 10, were recovered from 20 analyzed grains.

Sample 6-14 is a banded gneiss with plagioclase-rich bands alternating with garnet + plagioclase + kyanite/sillimanite + quartz + biotite ± muscovite layers. Prismatic zircon crystals up to 90 μm in length display 20–30 μm thick rims exhibiting oscillatory zoning overgrowing oscillatory zoned cores in CL. 33 of 62 analyses accepted by *TuffZirc* from zircon rims indicate a $^{206}Pb/^{238}U$ age of 437.9 + 8.6/−7.9 Ma with an average U/Th ratio of 38. 13 upper-intercept ages indicate exclusively Meso–Paleoproterozoic zircon inheritance of low U/Th cores with ages ranging from 920 to 2170 Ma and peaks at ~1300 and 1700–1800 Ma.

Sample 6-24 is from a variably deformed, 10 m thick, syn-post kinematic granitic dike that cuts regional foliation associated with the previous Jættedal complex samples (Fig. 3D). The analyzed sample was collected from a discontinuous, E–W striking mylonitic shear zone that cuts the dike with top-N fabrics defined by N-trending stretching lineations, S–C fabrics, and oblique subgrain foliation in quartz ribbons. Separated zircons are prismatic crystals 100–200 μm in length and exhibit oscillatory zoning with dark outermost rims in

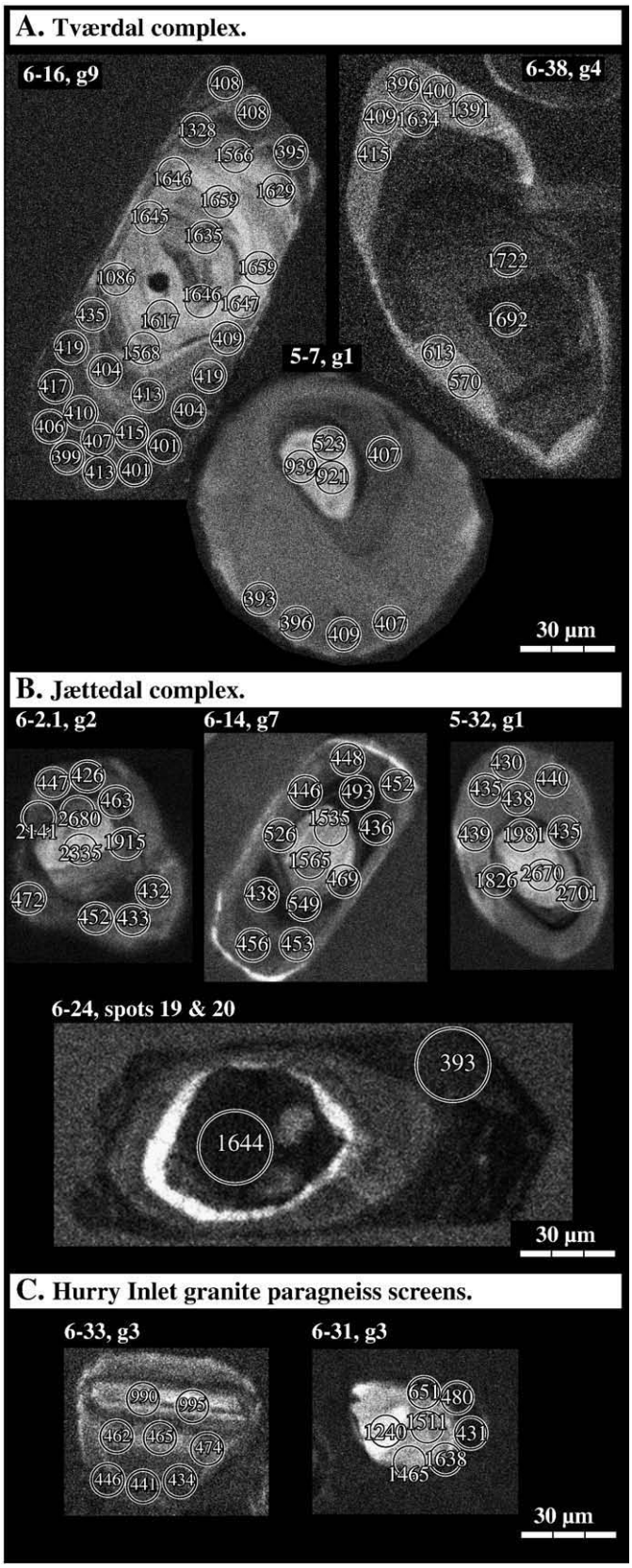

Fig. 4. Representative CL images illustrating core-to-rim chemical zoning and corresponding spot ages for zircons from A) the Tværdal complex, B) the Jættedal complex, and C) the paragneiss screens of the Hurry Inlet granite batholith. Spot ages reported in this figure are $^{206}Pb/^{238}U$ ages for analyses younger than 1000 Ma and are $^{206}Pb/^{207}Pb$ ages for analyses older than 1000 Ma. Images were acquired using the Cameca CAMSCAN Series II SEM at the University of Arizona.

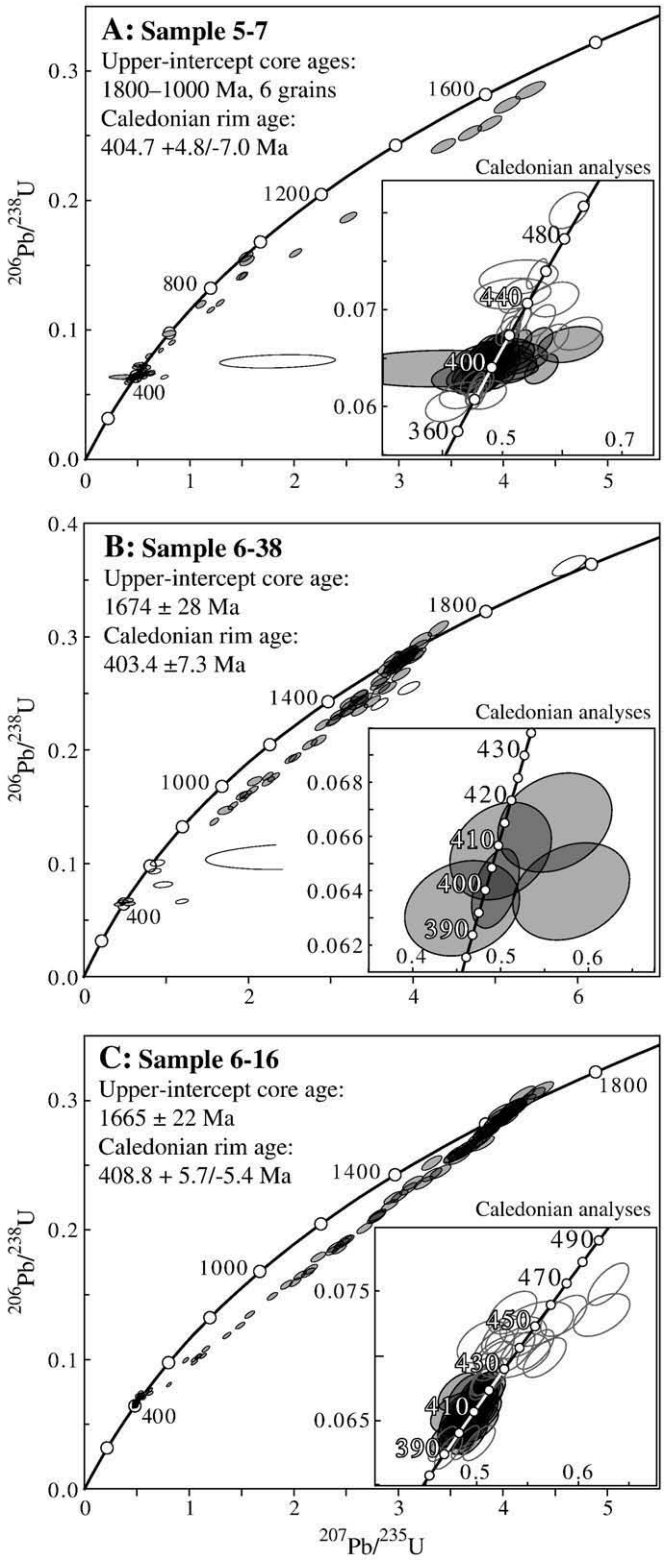

Fig. 5. U–Pb data from the Tværdal complex; inset plots show details of Caledonian analyses used to calculate Caledonian rim ages. Upper-intercept and Caledonian rim ages are reported at the 95% confidence level and calculated from analyses indicated by filled ellipses. Open ellipses were omitted by the *Tuffzirc* algorithm of Ludwig (2003) due to either inheritance or Pb loss. Error ellipses are shown at 1σ.

CL. Instrument scheduling prohibited this sample from being analyzed using the small-volume technique, although the relatively larger size of chemical domains in this sample allowed successful characterization using a larger laser spot size of 25 μm and following the procedure of Gehrels et al. (2008). 13 of 17 analyses from rims with U/Th ratios ranging from 1.4 to 53.9 yield a *TuffZirc* $^{206}Pb/^{238}U$ age of 393.5 + 13.0/−8.4 Ma. Core analyses, typically with U/Th ratios < 10, suggest inheritance of Mesoproterozoic zircons with peaks at ~1000, 1400, and 1600–1700 Ma.

4.3. Hurry Inlet granite

Zircons from two paragneisses within a screen near Kalkdal were analyzed from the Hurry Inlet granite (Figs. 7, 8, Table 1). Sample 6-31 is a retrogressed garnet + sillimanite + quartz + plagioclase ± muscovite gneiss found within a series of interlayered gneisses with various pelitic–psammitic compositions. Separated zircons are rounded to prismatic crystals 30–60 μm in diameter, and in CL, display a variety of core morphologies with dark rims <20 μm thick. Due to high U concentrations and resultant high Pb concentrations in zircon rims, many of the analyses in this sample were executed using a laser pulse rate of 2 Hz (rather than the standard 4 Hz) in order to avoid tripping the Channeltron detectors measuring Pb isotopes. Despite this difficulty, analyses of R33 at 2 and 4 Hz during the analysis session yield statistically equivalent $^{206}Pb/^{238}U$ weighted average ages of 408.9 ± 10.0 and 413.9 ± 8.5 Ma, respectively, and indicate that changing the laser hit rate did not affect the precision or accuracy of the technique beyond 1–2%. Zircon rims from sample 6-31 have an average U/Th ratio of 116, and 14 of 22 analyses accepted by *TuffZirc* indicate a $^{206}Pb/^{238}U$ age of 431.7 + 11.4/−8.0 Ma. Zircon cores typically have U/Th ratios < 5, and 25 upper-intercept ages indicate predominantly Proterozoic zircon inheritance with ages ranging from 1950 to 1000 Ma.

Sample 6-33 is a garnet-bearing granitic gneiss with minor biotite, muscovite and kyanite that is the dominant rock type exposed in the Kalkdal screen. Separated zircons are rounded to prismatic grains up to 60 μm in length, and in CL, display prismatic cores with oscillatory zoning overgrown by homogenously dark rims up to 20 μm thick that are best developed parallel to the long axis of prism cores. Rims yield an average U/Th ratio of 30 and a *TuffZirc* $^{206}Pb/^{238}U$ age of 417.5 + 9.1/−6.8 Ma from 26 of 49 analyses. Inherited cores have U/Th ratios that are typically < 10, and upper-intercept ages are predominantly Proterozoic with 13 grains ranging from 950 to 1950 and probability peaks at 1100 and 1600 Ma. One grain exhibits two distinct mixing lines that indicate a ~2400 Ma core and a ~1150 Ma mantle.

5. Discussion

5.1. The Liverpool Land tectonostratigraphy and regional correlations

The new mapping and U–Pb zircon data can be used to define the Liverpool Land tectonostratigraphy, and to place these rocks in the orogenic framework of the Laurentian–Baltican Caledonides. In the following discussion, upper-intercept ages are interpreted to indicate ages inherited from either detrital or primary magmatic cores, while ages from zircon rims, typically with high U/Th values—commonly associated with metamorphic zircons (e.g., Rubatto, 2002)—are interpreted to represent the timing of Caledonian metamorphism.

The Jættedal complex paragneisses and the screens of the Hurry Inlet granite are dominated by primarily late Paleo–Mesoproterozoic detrital zircon populations, and the youngest grains indicate maximum depositional ages of 920 ± 150 Ma and 950 ± 90 Ma, respectively (Table 1). These detrital signatures suggest direct correlation to either the Krummedal sequence or the Eleonore Bay Supergroup found in the inland fjords farther to the west (Fig. 8, Strachan et al., 1995; Kalsbeek et al., 2000; Watt et al., 2000; Leslie and Nutman, 2003). The Krummedal and Eleonore Bay Supergroup are part of a series of Neoproterozoic basins found in the north Atlantic that are dominated by late Paleo–Mesoproterozoic detritus thought to have

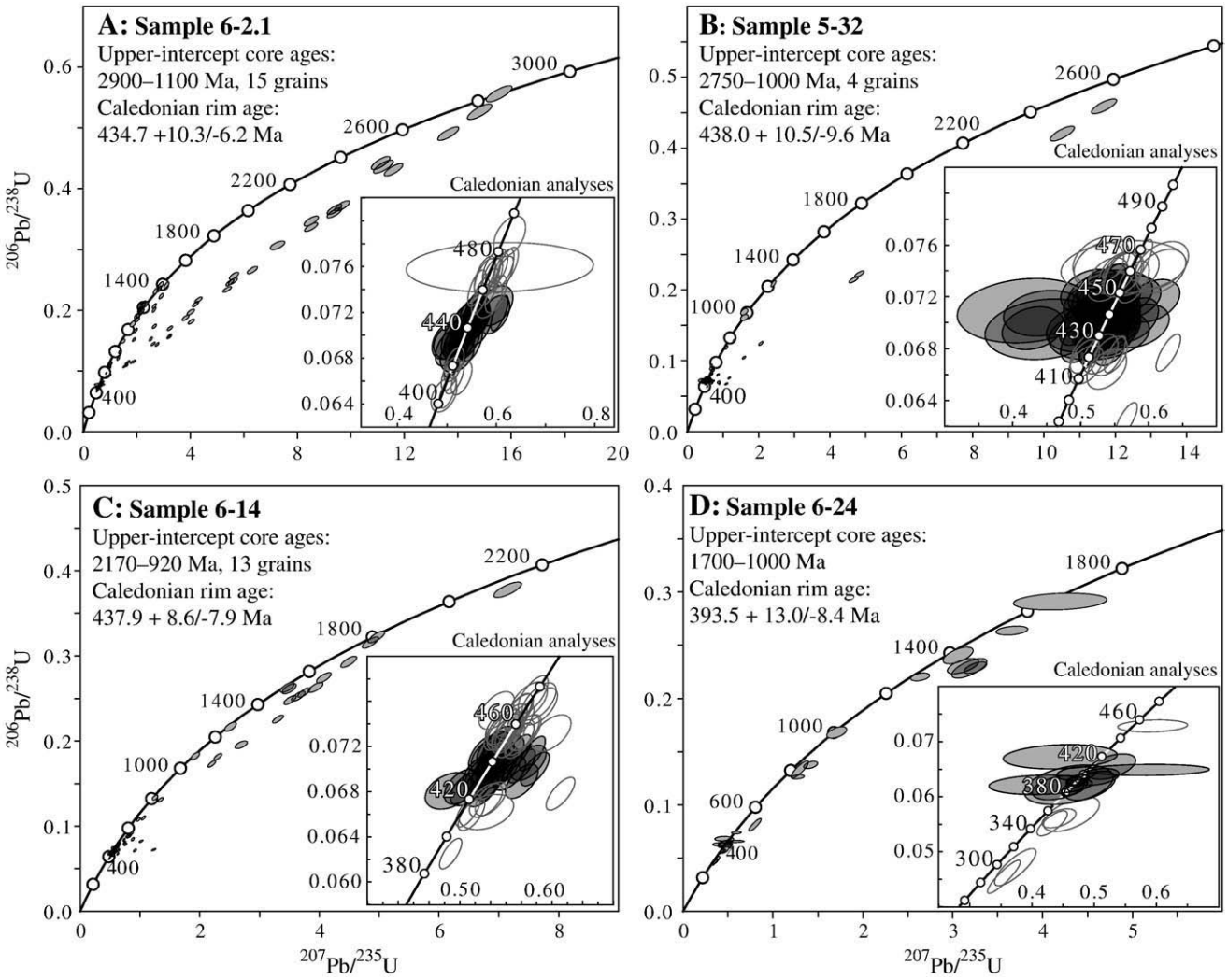

Fig. 6. U–Pb data from the Jættedal complex; inset plots show details of Caledonian analyses used to calculate Caledonian rim ages. Upper-intercept and Caledonian rim ages are reported at the 95% confidence level and calculated from analyses indicated by filled ellipses. Open ellipses were omitted by the *Tuffzirc* algorithm of Ludwig (2003) due to either inheritance or Pb loss. Error ellipses are shown at 1σ.

been derived from a Laurentia–Baltica source terrane (Cawood et al., 2007, and references therein), and deposited prior to, and during the opening of the Iapetus in a series of Rodinian intracontinental basins (Cawood et al., 2007), or on the Rodinian margin (Kirkland et al., 2007). While significant volumes of 1400–1100 Ma detritus—ages that are absent in Baltican source terranes—links these basins to Laurentia, the conspicuous absence of Archean detrital ages may indicate that the East Greenland sedimentary successions are allochthonous terranes emplaced on older Archean–Paleoproterozoic basement during subsequent deformation (Watt and Thrane, 2001). However, the relative lack of Archean grains may also be explained by minimal erosion of Archean terranes in the continental interior during deposition while Grenvillian uplift lead to widespread erosion of Mesoproterozoic source terranes along the southern margin of Rodinia (Cawood et al., 2007; Kirkland et al., 2007). This later hypothesis is supported by voluminous Archean detritus in Jættedal complex sample 6-2.1 that indicates Archean source terranes for at least some of the East Greenland sedimentary rocks. Archean detritus in the East Greenland Neoproterozoic basins could be related to variable provenance associated with subtle changes in sedimentary facies, or may indicate that the East Greenland basins are a series of successor basins comparable to the age-equivalent Torridonian succession of NW Scotland that includes older pre-Grenvillian sedimentary rocks that are dominated by Archean detritus and unconformably overlain by younger post-Grenvillian basins that display dominantly late Paleo–Mesoproterozoic provenance (Kinnaird et al., 2007).

The Jættedal paragneisses and screens of the Hurry Inlet granite also display similar ages for Caledonian metamorphism of 438–435 Ma and 432–417 Ma, respectively. Although Gilotti and McClelland (2005) showed that zircon ages in the Greenland Caledonides are susceptible to inheritance, the number of analyses involved in the calculations, concordia patterns, and the tight cluster of ages, particularly within the Jættedal complex, suggest that these ages represent the true timing of peak metamorphism. Furthermore, these metamorphic ages generally overlap with the emplacement of the Hurry Inlet granite from 445 to 423 Ma (Hansen and Steiger, 1971; Coe, 1975; Hartz et al., 2005; Augland, 2007), and with the 445–420 Ma metamorphism, anatexis and plutonism in the Krummedal of the HBTS (Strachan et al., 1995; Watt et al., 2000; Hartz et al., 2001; Kalsbeek et al., 2001; White et al., 2002) and lower-pressure metamorphism and plutonism in the lowermost levels of the Eleonore Bay Supergroup in the Franz Joseph Allochthon (Kalsbeek et al., 2001; Andresen et al., 2007). In the inland fjords, the amphibolite–granulite-facies Krummedal and the low-grade Eleonore Bay Supergroup can be distinguished by metamorphic

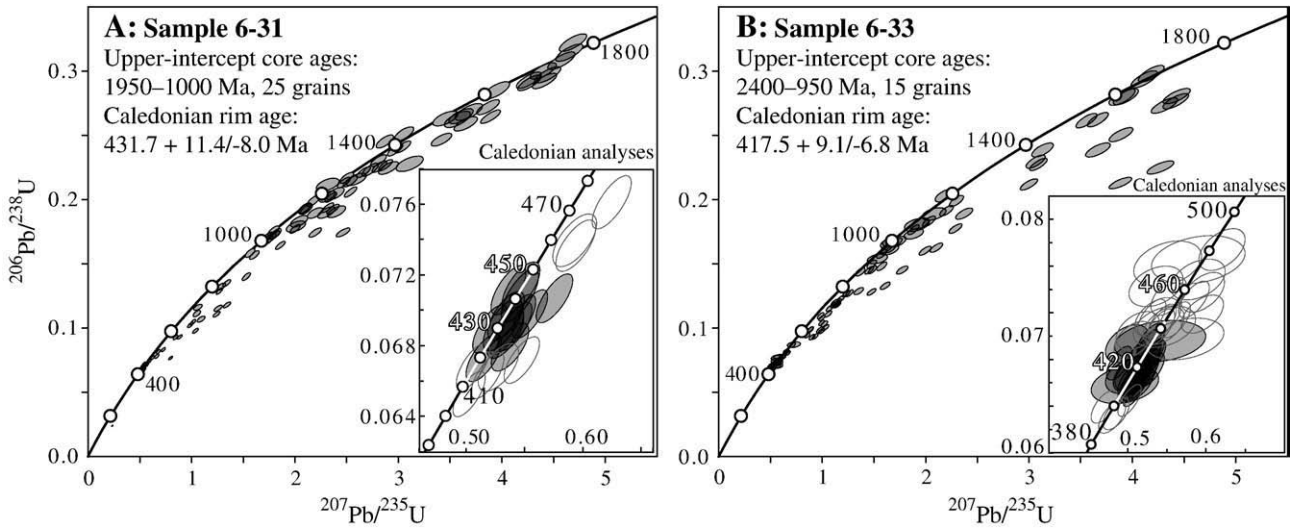

Fig. 7. U–Pb data from the paragneiss screens of the Hurry Inlet granite; inset plots show details of Caledonian analyses used to Caledonian rim ages. Upper-intercept and Caledonian rim ages are reported at the 95% confidence level and calculated from analyses indicated by filled ellipses. Open ellipses were omitted by the *Tuffzirc* algorithm of Ludwig (2003) due to either inheritance or Pb loss. Error ellipses are shown at 1σ.

grade and ~940–910 Ma plutonism that is widespread throughout the Krummedal and absent from the younger sedimentary rocks of the Eleonore Bay Supergroup (e.g., Higgins et al., 2004). In Liverpool Land, no evidence of late-Grenvillian plutonism has been documented, and thus, the interpretation that the Jættedal paragneisses and the screens of the Hurry Inlet granite may represent high-grade equivalents to the sedimentary rocks of the Eleonore Bay Supergroup and the Franz Joseph Allochthon cannot be ruled out. However, we correlate both the Jættedal paragneisses and the screens of the Hurry Inlet granite with the Krummedal sequence of the HBTS based on metamorphic grade, coincidence with early Caledonian metamorphism and plutonism, and the lack of associated low-grade Neoproterozoic sedimentary rocks. Regardless of this correlation, ~440–420 Ma anatexis in the Liverpool Land paragneisses links these rocks to the Laurentian overriding plate of the Caledonides as the Norwegian basement and allochthons of Baltican affinity are generally not characterized by high-grade deformation during this time interval (e.g., Brueckner and van Roermund, 2004).

Although the Jættedal paragneisses and the screens of the Hurry Inlet granite are both tentatively correlated with the Krummedal sequence, geologic mapping indicates that these two units are separated by the GSZ and occupy different tectonostratigraphic levels in Liverpool Land. This mapping is confirmed by the 393 Ma age on the granitic dikes that cuts layering in the Jættedal paragneisses. Top-N shear fabrics found in this sample, and in similar granitic dikes throughout the area, indicate that the Jættedal complex must have been in the ductilely deforming footwall of the GSZ during top-N displacement, as ductile top-N fabrics are absent from the older Hurry Inlet granites that occupy the hangingwall.

In contrast to the Jættedal complex paragneisses and the screens of the Hurry Inlet granite, the Tværdal complex gneisses indicate metamorphism at 409–403 Ma associated with burial 10–30 Myr after the timing of metamorphism in the Liverpool Land paragneisses. The ages recorded in the Tværdal complex gneisses are slightly older than 399–393 Ma zircon ages recorded in eclogites (Hartz et al., 2005; Augland, 2007), and may be the result of inheritance or temporal differences in zircon growth related to metamorphic reactions in the respective protoliths. Although 410–390 Ma high-pressure metamorphism is also observed farther north in Greenland, mantle peridotites have not been found in the North-East Greenland eclogite province (Gilotti and Krogh Ravna, 2002). Instead, ~400 Ma high-pressure metamorphism closely associated with garnet peridotites in the Tværdal complex is reminiscent of relationships observed throughout the subducted margin of Baltica currently exposed in the Western Gneiss Region of the Norwegian Caledonides (e.g., Brueckner and van Roermund, 2004). Furthermore, zircons from the Tværdal complex orthogneisses indicate protolith magmatic ages of ~1670 Ma, which coincide with ~1660 Ma zircon inheritance in a Tværdal complex eclogite that is interpreted to represent the original timing of mafic dike emplacement (Augland, 2007). Protolith ages younger than 1750 Ma have not been found elsewhere in Greenland, and the basement gneisses of North-East Greenland, the NSTS, HBTS and the Foreland are exclusively Paleoproterozoic–Archean (Thrane, 2002; Thrane, 2004; Kalsbeek et al., 2008). The ~1670–1660 Ma protolith ages from the Tværdal complex are more similar to Gothian plutonism from 1690 to 1630 Ma that is widespread throughout the Western Gneiss Region of Norway (Tucker et al., 1990; Skår, 2000; Austrheim et al., 2003), and once again suggests a direct correlation between the Tværdal complex and the western margin of Baltica. It is possible that Baltican rocks could have been emplaced within Laurentia during Grenvillian orogenesis, although the absence of Grenvillian zircon growth or Pb loss in Tværdal complex orthogneisses argues against this possibility. Although additional geochronology and isotopic work comparing the basement units of the inland fjords to the Tværdal complex must be completed to rule out the possibility that Tværdal complex is associated with Laurentia, our geochronology supports the hypothesis that the Tværdal complex represents a fragment of Baltican crust injected into the Laurentian overriding plate during Caledonian deformation (Smith and Cheeney, 1981; Augland, 2007). This correlation and the distinct difference in the timing of metamorphism between the Tværdal and Jættedal complexes requires that the contact between the Tværdal and Jættedal complexes—named the Ittoqqortoormiit shear zone herein—represents a profound tectonostratigraphic-bounding structure.

5.2. Implications for the dynamics of continental orogenesis

The correlation of the Tværdal complex with Baltica provides geochronologic evidence for a Laurentia–Baltica suture, and highlights underplating of the overriding plate by continental crust from the subducting plate as a significant process associated with continental orogenesis. Based on seismic, structural and analogue modeling studies of the Himalaya–Tibet orogen, regional-scale continental underplating has been proposed to occur as subducted continental

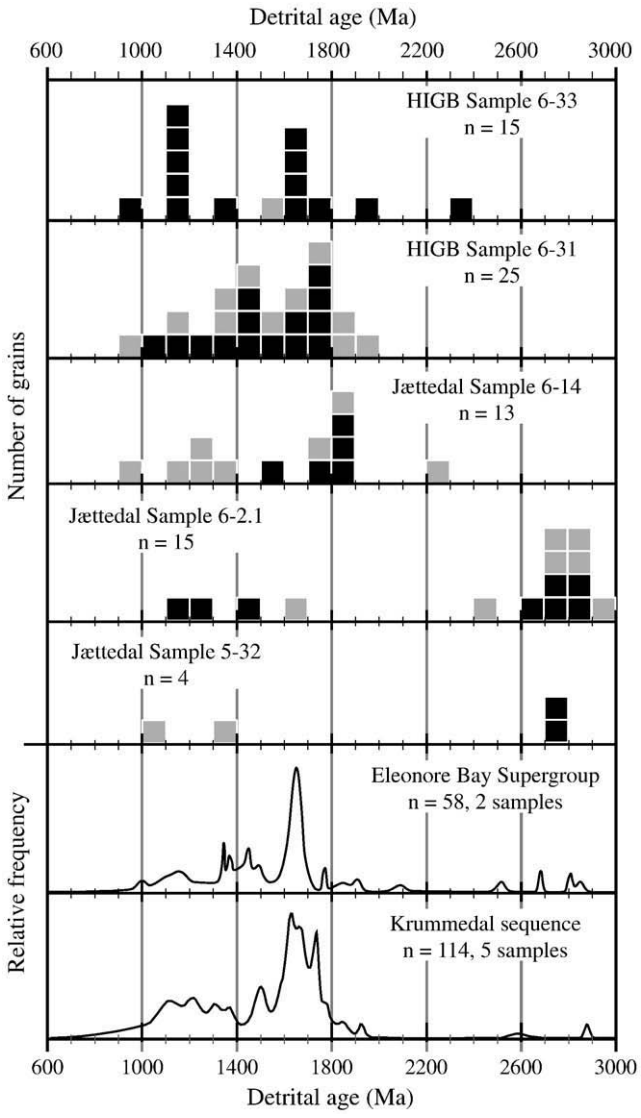

Fig. 8. Histograms illustrating the ages of detrital cores from the screens to the Hurry Inlet granite and the Jættedal complex. Solid black boxes indicate ages calculated with Caledonian lower-intercept anchor and multiple discordant core analyses, while grey boxes indicate ages calculated with Caledonian lower-intercept anchor and single discordant core analysis. Probability density function of detrital ages from the Eleonore Bay Supergroup (Watt et al., 2000) and the Krummedal sequence (Strachan et al., 1995; Watt et al., 2000; Leslie and Nutman, 2003) are shown for comparison.

Table 1
Upper-intercept ages from Liverpool Land detrital samples.

Grain	Age ± 95% (Ma)[a]	Anal. used[b]	MSWD	Grain	Age ± 95% (Ma)[a]	Anal. used[b]	MSWD
Paragneiss screens of the HIGB				Jættedal Complex paragneisses			
6-31				6-2.1			
31	977 ± 180	1	0.0	1	1132 ± 50	8	0.2
1	1052 ± 40	4	0.3	5	1200 ± 52	7	0.3
2	1135 ± 51	3	0.1	8	1402 ± 83	5	2.6
30	1146 ± 71	1	0.0	9	1623 ± 60	1	0.0
6	1201 ± 36	4	0.2	11	2447 ± 62	1	0.0
13	1315 ± 42	2	0.3	10	2607 ± 39	3	1.5
29	1360 ± 53	1	0.0	2	2711 ± 69	4	1.9
15	1382 ± 68	1	0.0	15	2716 ± 67	1	0.0
20	1419 ± 59	1	0.0	3	2721 ± 69	11	13.0
7	1435 ± 150	3	2.1	4	2726 ± 50	1	0.0
11	1453 ± 35	2	0.0	6	2827 ± 44	9	4.7
14	1459 ± 150	3	4.7	19	2841 ± 81	1	0.0
12	1517 ± 29	3	0.4	7	2856 ± 42	2	0.2
19	1548 ± 83	1	0.0	12	2872 ± 42	1	0.0
3	1607 ± 43	4	0.7	14	2903 ± 55	1	0.0
26	1632 ± 80	1	0.0	5-32			
18	1638 ± 53	2	0.1	8	1024 ± 270	1	0.0
24	1710 ± 45	2	0.2	4	1327 ± 70	1	0.0
9	1713 ± 100	3	2.1	2	2723 ± 34	2	0.5
10	1756 ± 53	5	2.1	1	2724 ± 30	3	0.1
4	1767 ± 50	1	0.0	6-14			
21	1784 ± 32	3	1.1	21	928 ± 150	1	0.0
23	1827 ± 48	1	0.0	15	1114 ± 110	1	0.0
22	1836 ± 84	1	0.0	13	1235 ± 130	1	0.0
17	1944 ± 59	1	0.0	11	1268 ± 110	1	0.0
6-33				18	1303 ± 110	1	0.0
3	960 ± 90	2	0.1	7	1558 ± 52	3	0.4
10	1109 ± 45	4	0.6	1	1703 ± 45	3	1.3
9	1109 ± 110	5	2.2	20	1771 ± 64	1	0.0
6	1119 ± 46	6	1.2	8	1823 ± 53	2	0.9
7[c]	1153 ± 39	7	1.3	10	1824 ± 38	2	0.4
15	1156 ± 45	7	1.5	5	1824 ± 30	4	0.9
13	1322 ± 37	5	0.9	4	1858 ± 53	1	0.0
4	1589 ± 81	1	0.0	6	2212 ± 55	1	0.0
5	1623 ± 82	5	2.6				
8	1649 ± 48	3	0.7				
11	1679 ± 37	3	0.5				
12	1680 ± 25	6	0.4				
14	1785 ± 38	4	0.9				
1	1947 ± 25	5	0.2				
7	2388 ± 38	2	1.7				

[a] Ages are upper-intercept model 1 ages calculated by Isoplot (Ludwig, 2003) with a Caledonian lower-intercept anchor.
[b] Indicates the number of analyses used in conjunction with the Caledonian anchor in the calculation of the upper-intercept age.
[c] Age derived from zircon mantle.

crust is underthrust beneath continental crust of the overriding plate following prior thinning or removal of the overriding plate mantle lithosphere (e.g., Owens and Zandt, 1997; DeCelles et al., 2002), or beneath the overriding plate mantle lithosphere followed by subsequent foundering of the overriding plate mantle lithosphere and replacement by the underplated continental crust (e.g., Chemenda et al., 2000). Both of these models are associated with wholesale foundering of the overriding plate mantle lithosphere and with regional uplift of overriding plate continental plateaux. Alternatively, continental underplating has also been suggested at more local scales with less of an influence on the regional evolution of the overriding plate. Local-scale underplating may be associated with isolated diapirs that rise from the downgoing slab through the mantle wedge (Yin et al., 2007), or limited underthrusting of neutrally buoyant continental crust subducted beneath the overriding plate as it spreads laterally at the Moho following exhumation from mantle depths (Walsh and Hacker, 2004). The apparently small areal extent of the Tværdal complex suggests that local-scale models for continental underplating are more applicable to the Greenland Caledonides, although additional regional geochronologic, isotopic and correlation studies are necessary to rigorously define the extent of the Tværdal complex and test this hypothesis.

Regardless of continental affinity, the metamorphic history of the Tværdal complex and its juxtaposition with the Jættedal complex across the Ittoqqortoormiit shear zone challenges traditional models for the exhumation of high-pressure terranes. Most high-pressure continental terranes are thought to have been exhumed from mantle depths to upper-crustal levels within the subduction channel and in the footwall position with respect to lithospheric-scale normal faults that act in concert with pure shear flattening and/or basal thrust fault imbrication (e.g., Ernst et al., 2007). In Liverpool Land, the Ittoqqortoormiit shear zone was responsible for juxtaposing the ~400 Ma eclogite-facies Tværdal complex with the ~440–420 Ma Jættedal complex at a position within the overriding plate rather than along a subduction zone. Furthermore, the relative position of the Ittoqqortoormiit shear zone in the footwall of the GSZ and its high-temperature fabrics that are overprinted and transposed by the normal-sense fabrics within the GSZ, indicates that the Ittoqqortoormiit shear zone was fundamentally

different, and active prior to the onset of displacement along the GSZ. Rather than single-stage exhumation along a lithospheric-scale normal fault, this suggests two phases of deformation associated with exhumation of the Tværdal complex: an initial phase of exhumation related to underplating and emplacement in the middle–lower crust along the Ittoqqortoormiit shear zone, followed by upper-crustal exhumation along the GSZ. $^{40}Ar/^{39}Ar$ muscovite cooling ages that range from 380 to 376 Ma in the footwall of the GSZ (Bowman, 2008) shortly after ~410–390 Ma metamorphism of the Tværdal complex suggest that arrival of the Tværdal Complex in the lower–middle crust via the Ittoqqortoormiit shear zone may have created a crustal instability in the overriding plate, and triggered crustal extension and the development of the GSZ. While the detailed kinematics and nature of the Ittoqqortoormiit shear zone remain enigmatic, the presence of two distinct structures in Liverpool Land supports multi-stage models for high-pressure exhumation that call for initial stages of deformation associated with underplating at mantle or lower crustal depths that trigger subsequent regional normal faulting and extension associated with upper-crustal exhumation (e.g., Walsh and Hacker, 2004; Johnston et al., 2007).

6. Conclusions

Mapping and zircon geochronology from Liverpool Land, East Greenland define three tectonostratigraphic units that are, from the bottom up, the Tværdal complex, the Jættedal complex and the Hurry Inlet granite. The Jættedal complex and the paragneiss screens of the Hurry Inlet granite share similar depositional and 440–420 Ma mid–lower crustal metamorphic histories, and are both correlated with the Krummedal sequence of the HBTS thrust sheet. In contrast, the Tværdal complex is characterized by burial to eclogite-facies from 410 to 393 Ma, and ~1670 Ma protolith ages that allow correlation to the subducted margin of Baltica. Initial juxtaposition of the Tværdal complex against the Jættedal complex in the lower–middle crust was accomplished along the Ittoqqortoormiit shear zone and closely followed by further exhumation into the upper crust of both the Tværdal and Jættedal complexes via normal-sense displacement along the GSZ. This work highlights the importance that continental underplating plays in the evolution of overriding plates during continental collisions, and supports multi-stage models for exhumation of high-pressure terranes.

Acknowledgments

Funding for field work in Greenland was supported by the Norwegian Science Council through the Petromaks program and a “Centre of Excellence” grant to Physics of Geological Processes. Aka Lynge and Luc Mehl are thanked for assistance with field logistics and field work. Post-doctoral support for Johnston while at the University of Arizona was supported by NSF EAR 044387 and 0732436 awarded to Gehrels. This manuscript benefitted from two detailed anonymous reviews.

Appendix A. Supplementary data

Supplementary data associated with this article can be found, in the online version

References

Andresen, A., Rehnström, E.F., Holte, M., 2007. Evidence for simultaneous contraction and extension at different structural levels during the Caledonian orogeny in NE Greenland. J. Geol. Soc. Lond. 164, 869–880.
Augland, L., 2007. The Gubbedalen Shear Zone; a terrane boundary in the East Greenland Caledonides. MS Thesis Thesis, University of Oslo, Norway, 126 pp.
Austrheim, H., Corfu, F., Bryhni, I., Andersen, T.B., 2003. The Proterozoic Hustad igneous complex: a low strain enclave with a key to the history of the Western Gneiss Region of Norway. Precambrian Res. 120, 149–175.
Barazangi, M., Ni, J., 1982. Velocities and propagation characteristics of Pn and Sn beneath the Himalayan Arc and Tibetan Plateau; possible evidence for under-thrusting of Indian continental lithosphere beneath Tibet. Geology 10, 179–185.
Bengaard, H.J. and Watt, W.S., 1986. 70 Ø.1 Syd, Kap Brewster; 1:100, 000; 70°30′N–70°00′N; 23°39′W–21°18′W, 1:100, 000. Geological Survey of Denmark and Greenland, pp. 70°30′N–70°00′N; 23°39′W–21°18′W.
Bird, P., 1991. Lateral extrusion of lower crust from under high topography, in the isostatic limit. J. Geophys. Res. 96, 10275–10286.
Black, L.P., et al., 2004. Improved 206Pb/238U microprobe geochronology by the monitoring of a trace-element-related matrix effect; SHRIMP, ID–TIMS, ELA–ICP–MS and oxygen isotope documentation for a series of zircon standards. Chem. Geol. 205, 115–140.
Bowman, D.R., 2008. Exhumation History of Caledonian Eclogites in Liverpool Land, East Greenland, and Comparisons with Eclogites in Norway. MS Thesis Thesis, Auburn University, 85 pp.
Brueckner, H.K., van Roermund, H.L.M., 2004. Dunk tectonics: a multiple subduction/eduction model for the evolution of the Scandinavian Caledonides. Tectonics 23, TC2004. doi:10.1029/2003TC001502.
Buchanan, J., 2008. Tectonic Evolution of a Caledonian-Aged Continental Basement Eclogite Terrane in Liverpool Land, East Greenland. MS Thesis Thesis, Auburn University, 106 pp.
Carswell, D.A., Brueckner, H.K., Cuthbert, S.J., Mehta, K., O'Brien, P.J., 2003. The timing of stabilisation and the exhumation rate for ultra-high pressure rocks in the Western Gneiss Region of Norway. J. Metamorph. Geol. 21, 601–612.
Cawood, P.A., Nemchin, A.A., Strachan, R.A., Prave, T., Krabbendam, M., 2007. Sedimentary basin and detrital zircon record along East Laurentia and Baltica during assemby and breakup of Rodinia. J. Geol. Soc. Lond. 164, 257–275.
Cheeney, R.F., 1985. The plutonic igneous and high-grade metamorphic rocks of southern Liverpool Land, central East Greenland, part of a supposed Caledonian and Precambrian complex. Rapp. Grønl. Geol. Unders. 123, 1–39.
Chemenda, A.I., Burg, J.-P., Mattauer, M., 2000. Evolutionary model of the Himalaya–Tibet system: geopoem: based on new modelling, geological and geophysical data. Earth Planet. Sci. Lett. 174, 397–409.
Coe, K., 1975. The Hurry Inlet granite and related rocks of Liverpool Land, East Greenland. Bull. Grønl. Geol. Unders. 115, 1–34.
Dallmeyer, R.D., Strachan, R.A., Henriksen, N., 1994. 40Ar/39Ar mineral age record in NE Greenland: implications for tectonic evolution fo the North Atlantic Caledonides. J. Geol. Soc. Lond. 151, 615–628.
DeCelles, P.G., Robinson, D.M., Zandt, G., 2002. Implications of shortening in the Himalayan fold-thrust belt for uplift of the Tibetan Plateau. Tectonics 21. doi:10.1029/2001TC001322.
Elvevold, S., Thrane, K., Gilotti, J.A., 2003. Metamorphic history of high-pressure granulites in Payer Land, Greenland Caledonides. J. Metamorph. Geol. 21, 49–63.
England, P.C., Houseman, G.A., 1989. Extension during continental convergence, with application to the Tibetan plateau. J. Geophys. Res. 94, 17,561–17,579.
Ernst, W.G., Hacker, B.R., Liou, J.G., 2007. Petrotectonics of ultrahigh-pressure crustal and upper-mantle rocks—implications for Phanerozoic collisional orogens. Geol. Soc. Am. Spec. Pap. 443, 27–49. doi:10.1130/2007.2433(02.
Friderichsen, J.D. and Surlyk, F., 1981. 70 Ø.1 Nord, Hurry Inlet; 1:100, 000; 71°00′N–70°30′N; 23°39′W–21°18′W. Geological Survey of Denmark and Greenland.
Gee, D.G., 1975. A tectonic model for the central part of the Scandinavian Caledonides. Am. J. Sci. 275-A, 468–515.
Gehrels, G., Valencia, V.A., Ruiz, J., 2008. Enhanced precision, accuracy, efficiency, and spatial resolution of U–Pb ages by laser ablation–multicollector–inductively coupled plasma–mass spectrometry. Geochem. Geophys. Geosyst. 9 (3). doi:10.1029/2007GC001805.
Gerya, T.V., Perchuk, L.L., Burg, J.-P., 2008. Transient hot channels: Perpetrating and regurgitating ultrahigh-pressure, high-temperature crust–mantle associations in collisional belts. Lithos 103, 236–256.
Gilotti, J.A., Elvevold, S., 2002. Extensional exhumation of high-pressure granulite terrane in Payer Land, Greenland Caledonides: structural, petrologic and geochronologic evidence from metapelites. Can. J. Earth Sci. 39, 1169–1187.
Gilotti, J.A., Krogh Ravna, E., 2002. First evidence for ultrahigh-pressure metamorphism in the North-East Greenland Caledonides. Geology 30, 551–554.
Gilotti, J.A., McClelland, W.C., 2005. Leucogranites and the time of extension in the East Greenland Caledonides. J. Geol. 113, 399–417.
Gilotti, J.A., McClelland, W.C., 2007. Characteristics of, and a tectonic model for, ultrahigh-pressure metamorphism in the overriding plate of the Caledonian Orogen. Int. Geol. Rev. 49, 777–797.
Gilotti, J.A., McClelland, W.C., 2008. Geometry, kinematics, and timing of extensional faulting in the Greenland Caledonides—a synthesis. In: Higgins, A.K., Gilotti, J.A., Smith, M.P. (Eds.), The Greenland Caledonides: Evolution of the Northeast Margin of Laurentia: GSA Memoir 202, pp. 251–271. doi:10.1130/2008.1202(10).
Gilotti, J.A., Nutman, A.P., Brueckner, H.K., 2004. Devonian to Carboniferous collision in the Greenland Caledonides: U–Pb zircon and Sm–Nd ages of high-pressure and ultrahigh-pressure metamorphism. Contrib. Mineralog. Petrol. 148 (216–235).
Gilotti, J.A., Jones, K.A., Elvevold, S., 2008. Caledonian metamorhpic patterns in Greenland. In: Higgins, A.K., Gilotti, J.A., Smith, M.P. (Eds.), The Greenland Caledonides: Evolution of the Northeast Margin of Laurentia: GSA Memoir 202, pp. 201–225. doi:10.1130/2008.1202(08).
Hacker, B., et al., 2005. Near-ultrahigh pressure processing of continental crust: Miocene crustal xenoliths from the Pamir. J. Petrol. 46 (8), 1661–1687.
Haller, J., 1971. Geology of the East Greenland Caledonides. Interscience, London.
Hansen, B.T., Steiger, R.H., 1971. The geochronology of the Scorsbysund area. Progress report 1: Rb/Sr mineral ages. Rapp. Grønl. Geol. Unders. 37, 59–61.

Hartz, E., Andresen, A., 1995. Caledonian sole thrust of central east Greenland: a crustal-scale Devonian extensional detachment? Geology 23, 637–640.
Hartz, E., Andresen, A., Martin, M.W., Hodges, K.V., 2000. U–Pb and 40Ar/39Ar constraints on the Fjord Region Detachment Zone: a long-lived extensional fault in the central East Greenland Caledonides. J. Geol. Soc. Lond. 157, 795–809.
Hartz, E., Andresen, A., Hodges, K.V., Martin, M.W., 2001. Syncontractional extension and exhumation of deep crustal rocks in the east Greenland Caledonides. Tectonics 20, 58–77.
Hartz, E., Condon, D., Austrheim, H., Erambert, M., 2005. Rediscovery of the Liverpool Land eclogites (central East Greenland): a post and supra-subduction UHP province. Mitt. Österr. Mineralogischen Ges. 150, 50.
Henriksen, N., 1985. The Caledonides of central East Greenland 70 degrees–76 degrees N. In: Gee, D., Sturt, B.A. (Eds.), The Caledonide Orogen. Scandinavia and Related Areas. John Wiley, New York, pp. 1095–1113.
Henriksen, N., 2003. Caledonian Orogen, East Greenland 70°–82°N. Geological Map 1:1,000,000. Geological Survey of Denmark and Greenland, Copenhagen.
Higgins, A.K., Leslie, A.G., Smith, M.P., 2001. Neoproterozoic–Lower Paleozoic stratigraphical relationships in the marginal thin-skinned thrust belt of the East Greenland Caledonides: comparisons with the foreland in Scotland. Geol. Mag. 138 (2), 143–160.
Higgins, A.K., et al., 2004. The foreland-propagating thrust architecture of the East Greenland Caledonides, 72°–75°N. J. Geol. Soc. Lond. 161, 1009–1026.
Johnston, S.M., Hacker, B.R., Ducea, M., 2007. Exhumation of ultrahigh-pressure rocks beneath the Hornelen Segment of the Nordfjord–Sogn Detachment Zone, Western Norway. Geol. Soc. Am. Bull. 119, 1232–1248. doi:10.1130/B26172.1.
Johnston, S., Gehrels, G., Valencia, V., Ruiz, J., 2009. Small-volume U–Pb zircon geochronology by laser ablation–multicollector–ICP–MS. Chem. Geol. 259, 218–219. doi:10.1016/j.chemgeo.2008.11.004.
Jones, K.A., Escher, J.C., 2002. Near-isothermal decompression within a clockwise *P–T* evolution recorded in migmatitic mafic granulites from Clavering Ø, NE Greenland: implications for the evolution of the Caledonides. J. Metamorph. Geol. 20, 365–378.
Jones, K.A., Strachan, R.A., 2000. Crustal thickening and ductile extension in the NE Greenland Caledonides: a metamorphic record from anatectic pelites. J. Metamorph. Geol. 18, 719–735.
Kalsbeek, F., Thrane, K., Nutman, A.P., Jepsen, H.F., 2000. Late Mesoproterozoic to early Neoproterozoic history of the East Greenland Caledonides: evidence for Grenvillian orogenesis? J. Geol. Soc. Lond. 157, 1215–1225.
Kalsbeek, F., Jepsen, H.F., Nutman, A.P., 2001. From source migmatites to plutons: tracking the origin of ca. 435 Ma S-type granites in the East Greenland Caledonian orogen. Lithos 57, 1–21.
Kalsbeek, F., et al., 2008. Polyorogenic history of the East Greenland Calendonides. Geol. Soc. Am. Mem. 202, 55–72. doi:10.1130/2008.1202(03.
Kinnaird, T.C., et al., 2007. The late Mesoproterozoic–early Neoproterozoic tectonostratigraphic evolution of NW Scotland: the Torridonian revisited. J. Geol. Soc. Lond. 164, 541–551.
Kirkland, C.L., Daly, J.S., Whitehouse, M., 2007. Provenance and terrane evolution of the Kalak Nappe Complex, Norwegian Caledonides: implications for Neoproterozoic paleogeography and tectonics. J. Geol. 115 (21–41).
Krank, E.H., 1935. On the crystalline complex of Liverpool Land. Medd. Grønl. 95 (7), 1–122.
Leslie, A.G., Higgins, A.K., 1999. On the Caledonian (and Grenvillian) geology of Bartholin Land, Ole Rømer Land and adjacent nunataks, East Greenland. Danmarks and Grønlands Geologiske Undersøgelse Rapport, 1999/19, pp. 11–26.
Leslie, A.G., Nutman, A.P., 2003. Evidence for Neoproterozoic orogenesis and early high temperature Scandian deformation events in the southern East Greenland Caledonides. Geol. Mag. 3, 309–333.
Ludwig, K., 2003. User's Manual for Isoplot 3.00, A Geochronological Toolkit for Microsoft Excel. Berkeley Geochronology Center Special Publication, 4.
McClelland, W.C., Gilotti, J.A., 2003. Late-stage extensional exhumation of high-pressure granulites in the Greenland Caledonides. Geology 31 (3), 259–262.
McClelland, W.C., Power, S.E., Gilotti, J.A., Mazdab, F.K., Wopenka, B., 2006. U–Pb SHRIMP geochronology and trace-element geochemistry of coesite-bearing zircons, North-East Greenland Caledonides. Geol. Soc. Am. Spec. Pap. 403, 23–43. doi:10.1130/2006.2403(02).
Molnar, P., Tapponnier, P., 1975. Cenozoic tectonics of Asia: effects of a continental collision. Science 189, 419–426.
Owens, T.J., Zandt, G., 1997. Implications of crustal property variations for models of Tibetan plateau evolution. Nature 387, 37–43.
Rex, D.C., Higgins, A.K., 1985. Potassium–argon mineral ages from teh East Greenland Caledonides between 72 degrees and 74 degrees N. In: Gee, D., Sturt, B.A. (Eds.), The Caledonide Orogen—Scandinavia and Related Areas. John Wiley, New York, pp. 1115–1124.
Roberts, D., 2003. The Scandinavian Caledonides: event chronology, paleogeographic settings and likely modern analogues. Tectonophysics 365, 283–299.
Root, D.B., Hacker, B.R., Mattinson, J.M., Wooden, J.L., 2004. Young age and rapid exhumation of Norwegian ultrahigh-pressure rocks: an ion microprobe and chemical abrasion study. Earth Planet. Sci. Lett. 228, 325–341.
Rubatto, D., 2002. Zircon trace element geochemistry: partitioning with garnet and the link between U–Pb ages and metamorphism. Chem. Geol. 184, 123–138.
Sartini-Rideout, C., Gilotti, J.A., McClelland, W.C., 2006. Geology and timing of dextral strike–slip shear zones in Danmarkshavn, North-East Greenland Caledonides. Geol. Mag. 143, 431–446. doi:10.1017/S0016756806001968.
Skår, Ø., 2000. Field relations and geochemical evolution of the Gothian rocks in the Kvamsøy ara, southern Western Gneiss Region, Norway. Nor. Geol. Under. Bull. 437, 5–23.
Smith, D.C., Cheeney, R.F., 1981. A new occurrence of garnet–ultrabasite in the Caledonides: a Cr-rich chromite–garnet–lherzolite from Tvaerdalen, Liverpool Land, East Greenland. Terra Cognita 1 (1), 74.
Smith, M.P., Robertson, S., 1999. The Nathhorst Land Group (Neoproterozoic) of East Greenland — lithostratigraphy, basin geometry and tectonic history. Danmarks and Grønlands Geologiske Undersøgelse Rapport, 1999/19, pp. 127–143.
Strachan, R.A., Nutman, A.P., Friderichsen, J.D., 1995. SHRIMP U–Pb geochronology and metamorphic history of the Smallefjord sequence, NE Greenland Caledonides. J. Geol. Soc. Lond. 152, 779–784.
Thrane, K., 2002. Relationships between Archaean and Paleoproterozoic crystalline basement complexes in the southern part of the East Greenland Caledonides: and ion microprobe study. Precambrian Res. 113, 19–42.
Thrane, K., 2004. Palaeoproterozoic age of a basement gneiss complex in the Charcot Land tectonic window, East Greenland Caledonides. Geol. Surv. Denmark Greenland Bull. 6, 57–66.
Tucker, R.D., Krogh, T.E., Råheim, A., 1990. Proterozoic evolution and age-province boundaries in the central part of the Western Gneiss region, Norway: results of U–Pb dating of accessory minerals from Trondheimsfjord to Geiranger. In: Gower, C.F., Rivers, T., Ryan, B. (Eds.), Mid-Proterozoic Laurentia–Baltica. GAC special paper. Geological Association of Canada, St. John's (Newfoundland), pp. 149–173.
Walsh, E.O., Hacker, B.R., 2004. The fate of subducted continental margins: two-stage exhumation of the high-pressure to ultrahigh-pressure Western Gneiss complex, Norway. J. Metamorph. Geol. 22, 671–689.
Walsh, E.O., Hacker, B.R., Gans, P., Grove, M., Gehrels, G., 2007. Protolith ages and exhumation histories of (ultra)high-pressure rocks across the Western Gneiss Region, Norway. Geol. Soc. Am. Bull. 119 (3/4), 289–301. doi:10.1130/B25817.1.
Warren, C.J., Beaumont, C., Jamieson, R.A., 2008. Formation and exhumation of ultra-high-pressure rocks during continental collision: role of detachment in the subduction channel. Geochem. Geophys. Geosyst. 9. doi:10.1029/2007GC001839.
Watt, G.R., Thrane, K., 2001. Early Neoproterozoic events in East Greenland. Precambrian Res. 110, 165–184.
Watt, G.R., Kinny, P.D., Friderichsen, J.D., 2000. U–Pb geochronology of Neoproterozoic and Caledonian tectonothermal events in the East Greenland Caledonides. J. Geol. Soc. Lond. 157, 1031–1048.
White, A.P., Hodges, K.V., 2002. Multistage extensional evolution of the central East Greenland Caledonides. Tectonics 21. doi:10.1029/2001TC001308.
White, A.P., Hodges, K.V., 2003. Pressure–temperature–time evolution of the Central East Greenland Caledonides: quantitative constraints on crustal thickening and synorogenic extension. J. Metamorph. Geol. 21, 875–897.
White, A.P., Hodges, K.V., Martin, M.W., Andresen, A., 2002. Geologic constraints on middle-crustal behavior during broadly synorogenic extension in the central East Greenland Caledonides. Int. J. Earth Sci. 91, 187–208.
Wittlinger, G., et al., 2004. Teleseismic imaging of subduction lithosphere and Moho offsets beneath western Tibet. Earth Planet. Sci. Lett. 221, 117–130.
Yin, A., et al., 2007. Early Paleozoic tectonic and thermomechanical evolution of ultrahigh-pressure (UHP) metamorphic rocks in the Northern Tibetan Plateau, Northwest China. Int. Geol. Rev. 49, 681–716.